FACTA UNIVERSITATIS (NIŠ)
Series: Electronics and Energetics vol. 11, No.2 (1998), 207-221

AN APPLICATION OF SPHERICAL CODES TO POLARIZATION SHIFT KEYING MODULATION

Aleksandra Pižurica, Vojin Šenk and Veselin Pižurica

Abstract. A possibility of applying $3n$–dimensional spherical codes to polarization shift keying systems is investigated. Signal point constellations are optimized in a way that maximizes the minimum Euclidean distance. The potential improvement in system performance, resulting from the increase of signal space dimensionality, is verified through simulation. The possibility of extracting signal point constellations from lattice packings is also considered.

1. Introduction

Polarization Shift Keying (POLSK) is a form of digital optical modulation. It exploits vector characteristics of the lightwave carrier. Information is contained within the state of polarization (SOP) of a fully polarized lightwave. Demodulation and detection are based on Stokes parameters extraction at the receiver. A detailed theoretical treatment is presented in [1]. Since SOP provides three degrees of freedom, POLSK is especially suited for nonbinary transmission. An optimization of signal points constellations in Stokes space is performed in [2]. The fluctuations of the received field SOP, caused by fiber birefringence, are compensated using either active electro–optic control or polarization tracking algorithms [3] in order to recover the reference signal points. An alternative technique, which does not require the reference generation at the receiver, uses differential detection [4]. An important feature of POLSK is its robustness with respect to laser phase noise [5]. The use of equipower signal point constellations makes it less susceptible to nonlinear effects in optical fiber.

Manuscript received August 12, 1998.

Aleksandra Pižurica is with the University of Ghent, Dept. TELIN, Sint Pietersnieuwstr. 41, 9000 Gent, Belgium, E-mail: sanja@telin.rug.ac.be. Prof. dr Vojin Šenk is with the Faculty of Engineering, Trg D. Obradovica 6, 21000 Novi Sad, Yugoslavia. Veselin Pižurica is with the Free University of Brussels (VUB), Brussels, Belgium.

In this paper, we propose an application of a special class of spherical codes to polarization shift keying modulation. In standard POLSK applications, each symbol represents an appropriate polarization state, which is defined as a 3–tuple of Stokes parameters (s_1, s_2, s_3) in three–dimensional (3–D) Stokes space. In general, $3n$ dimensional signal space $(n = 1, 2, \dots)$ can be used for POLSK modulation. Increasing the dimensionality of the signal space leads to the reduction of error probability, having lightwave power and bandwidth occupation unchanged. The gain is achieved at the expense of an increased complexity at the receiver. The improvement in error probability is verified through simulations.

In Section 2 we give a brief overview of polarization of a monochromatic lightwave and explain the representation of SOP in the Stokes space and on the Poincaré sphere.

Basic principles of polarization modulation are discussed in Section 3.

In Section 4 we explain the application of $3n$ dimensional spherical codes to POLSK signas. In the absence of laser phase noise, the performance of different signal point constellations is well determined by Euclidean distance. $3n$–dimensional constellations with different numbers of signal points are optimized in that sense, but in a way which preserves constant power transmission. The possibility of applying lattice–based codes [6] is also examined.

The simulation method that we chose for obtaining numerical data for these codes is described in Section 5, and the simulation results thus obtained are presented and discussed in Section 6.

2. Theory

Let us suppose a fully polarized lightwave, which propagates in the z–axis direction of the Cartesian coordinate system. The electric field E can be decomposed into two orthogonal components, E_x and E_y

$$\begin{aligned} E &= E_x i_x + E_y i_y, \\ E_x &= a_x(t) e^{j(\omega t + \phi_x(t))}, \\ E_y &= a_y(t) e^{j(\omega t + \phi_y(t))}, \end{aligned} \tag{1}$$

SOP is fully determined by the amplitudes of these components, a_x and a_y, and their phase difference $\phi_y - \phi_x$. In optical communications the polarization state is usualy described using Stokes parameters. The Stokes parameters, in the general form, are defined as [7]

$$s_0 = E_x E_x^* + E_y E_y^*, \tag{2a}$$

$$s_1 = E_x E_x^* - E_y E_y^*, \tag{2b}$$

$$s_2 = E_x E_y^* + E_y E_x^*, \tag{2c}$$

$$s_3 = E_y E_x^* - E_x E_y^*, \tag{2d}$$

In the case of a fully polarized lightwave we have

$$s_0 = a_x^2 + a_y^2, \tag{3a}$$

$$s_1 = a_x^2 - a_y^2, \tag{3b}$$

$$s_2 = 2a_x a_y \cos\delta, \tag{3c}$$

$$s_3 = 2a_x a_y \sin\delta, \tag{3d}$$

where

$$\delta = \phi_y - \phi_x. \tag{4}$$

The Stokes parameter s_0 represents the total electromagnetic power of a lightwave. If the lightwave is fully polarized, as we suppose here, one can easily prove that

$$s_0^2 = s_1^2 + s_2^2 + s_3^3. \tag{5}$$

Therefore, only three out of four Stokes parameters are independent. A geometric representation of the polarization state on the surface of the so–called *Poinceré* sphere [7] is shown in Fig.1.

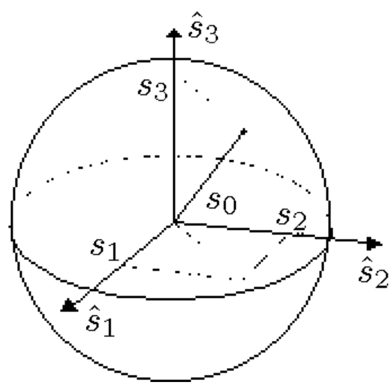

Figure 1. Representation of the polarization state on the Poinceré sphere.

Every polarization state of a lightwave with a given intensity (s_0 =const) corresponds to a point on the surface of the Poincaré sphere and vice versa. The upper half of the sphere corresponds to right oriented polarization states

($\sin\delta > 0$) and the lower half corresponds to left orientations ($\sin\delta < 0$). Circular polarizations with two opposite orientations correspond to the poles of the sphere. The right circular polarization ($a_x = a_y, \delta = \pi/2$) is presented by the point $s_1 = s_2 = 0$, $s_3 = s_0$, while the left circular polarization ($a_x = a_y$, $\delta = 3\pi/2$) corresponds to the point $s_1 = s_2 = 0$, $s_3 = -s_0$. All linear polarizations ($\delta = 0$ or $\delta = \pi$) are located on the equator of the Poinceré sphere.

3. Polarization modulation

Polarization modulation does not necessarily require constant power of the lightwave carrier. However, from the viewpoint of nonlinear effects in the optical fiber, it is most convenient to apply signaling with constant power. Some examples of signal point constellations with constant power are shown in Fig. 2. In the case of binary signaling, the symbols are two antipodal points on the surface of the Poincerè sphere (Fig. 2.a). The optimal constellation, in the sense of Euclidean distance, with four signal points is a tetrahedron (Fig. 2.b). A possible constellation with eight signal points is cube (Fig. 2.c), but it is not optimal in the sense of Euclidean distance [2], [8].

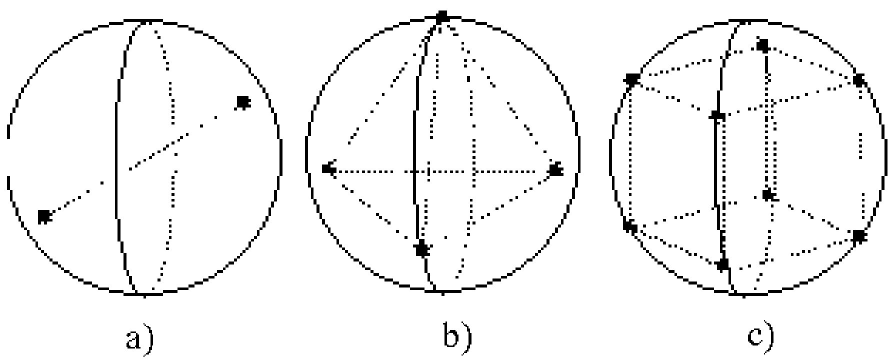

Figure 2. The examples of signal point constellations with constant power. a) 2–POLSK, b) 4–POLSK tetrahedron, c) 8–POLSK cube.

Optical fiber itself does not introduce polarization dependent losses. Depolarization effects can also be neglected, even after long distances (e.g. several hundreds of km) [9]. The output SOP in general fluctuates randomly [10], but the orthogonality between orthogonal input states is preserved. Therefore, the only influence of the monomode optical fiber is a rigid rotation of the signal point constellation in the Stokes space [2]. Reference signal points at the receiver are generated using either polarization tracking algorithms or active electro–optic control [1]. Polarization tracking can be implemented using relatively simple electronic processing [3] due to the fact that polarization fluctuations are slow as compared to the signaling rate. Another possibility is to use differential detection [4], which does not require the reference signal at the receiver, but at the expense of a slightly worse performanse.

Shematic representation of the coherent POLSK receiver, as proposed in [2], is given in Fig. 3.

A detailed analysis of the error probability in coherent POLSK systems is presented in [1] and [2]. Noise in the coherent receiver, including the local oscilator shot noise, is modeled as the white Gaussian noise.

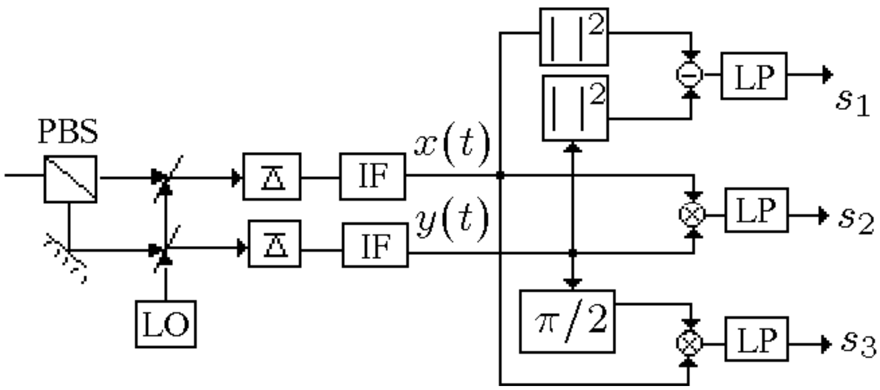

Figure 3. Schematic representation of a heterodyne coherent POLSK receiver [2]. PBS – polarization beam splitter, IF – intermediate filter, LP – low pass filter.

The complex envelopes of signals in two arms of the coherent receiver, after IF filtering, can be written as

$$\begin{aligned} x(t) &= a_x(t)e^{j\phi_x(t)} + n_x(t), \\ y(t) &= a_y(t)e^{j\phi_y(t)} + n_y(t), \end{aligned} \tag{6}$$

where

$$\begin{aligned} n_x &= n_{xc} + jn_{xs}, \\ n_y &= n_{yc} + jn_{ys}, \end{aligned} \tag{7}$$

n_{xc}, n_{xs}, n_{yc} and n_{ys} are Gaussian random processes with variance $\sigma^2 = N_0 B_{IF}$. $N_0/2$ is the power spectral density of the underlying white noise and BIF is the bandwidth of the IF filter. The error probability for binary POLSK is [1]

$$P_e = \frac{1}{2} \exp\left\{-\frac{s_0}{4\sigma^2}\right\}, \tag{8}$$

where the Stokes parameter s_0 represents the optical power of the signal. For M–ary POLSK, with regular signal point constellations (with identical decision regions for all the signal points) [2]

$$P_e = 1 - F_\theta(\theta_1) + \frac{n}{\pi} \int_{\theta_0}^{\theta_1} \arccos\left(\frac{\tan\theta_0}{\tan t}\right) f_\theta(t) dt, \tag{9}$$

where

$$f_\theta(t) = \frac{\sin t}{2} e^{-\frac{s_0}{4\sigma^2}(1-\cos t)} \left[1 + \frac{s_0}{4\sigma^2}(1 + \cos t)\right], \tag{10}$$

$$F_\theta(t) = 1 - \frac{1}{2} e^{-\frac{s_0}{4\sigma^2}(1-\cos t)} (1 = \cos t), \qquad t \in [0, \pi]. \tag{11}$$

n, θ_0 and θ_1 that appear in (9) are parameters of the chosen signal point constellation. They are tabulated for several regular poliedra in [2]. For the tetrahedron $n = 3$, $\theta_0 = [\pi - \arctan(2\sqrt{2}]/2$, $\theta_1 = \pi - 2\theta_0$ and for the cube $n = 3$, $\theta_0 = \arctan(1/\sqrt{2})$, $\theta_1 = \pi/2 - \theta_0$.

The influence of the laser phase noise is neglected, assuming that the IF filter bandwidth B_{IF} is wide enough to avoid parasite amplitude modulation [1], [2]. It should be noted that wider B_{IF} results in increased power of the filtered additive noise. This is partially compensated by applying low pass electrical filters, i.e. postdetection filters, as shown in Fig. 3. Postdetection filtering technique in POLSK systems is analyzed in detail in [5].

4. Spherical codes for POLSK signals

A signal point from the $3n$–dimensional space $X = (x_1, x_2, \ldots, x_{3n})$ could be transmitted as a combination of n SOP's in n consecutive signaling intervals. The first three elements of a given $3n$–tuple X would then represent the values of Stokes parameters during the first signaling period. In the next time interval, the SOP defined by the next three elements of X would be transmitted, and so on. Thus a $3n$–dimensional symbol is composed of n subsymbols representing different SOP's. At the receiver each SOP is independently detected and stored until the whole symbol is completed. The decision process is performed on $3n$–dimensional symbols using the maximum scalar product criterion.

A $3n$–dimensional spherical code is a subset of points of a $3n$–dimensional sphere. The coordinates of each signal point X satisfy

$$|X|^2 = x_1^2 + x_2^2 + \ldots + x_{3n}^2 = \text{const} \tag{12}$$

Spherical codes have been extensively studied in [6]. In the case considered here, we are interested in a special class of spherical codes that satisfy an additional condition

$$x_{3j+1}^2 + x_{3j+2}^2 + x_{3j+3}^2 = C, \qquad j = 0, 1, \ldots, n-1, \tag{13}$$

where C is an arbitrary constant. This constraint impies that all subsymbols are represented as SOP vectors lying on a constant radius sphere. Thus, equipower signal transmission is provided, which is important from the viewpoint of suppressing nonlinear effects in the optical fiber. For transmission of k input bits per signaling interval in a $3n$–dimensional signal space, $L = 2^{nk}$ different code words ($3n$–tuples) are needed.

$3n$–dimensional signal point constellations are optimized in the squared Euclidean distance sense, while preserving the constant power in each signaling period, according to Eq. (13). The optimization is performed using the iterative method of [11], which minimizes the generalized function

$$g(\{X_l\}) = \sum_{l=2}^{L} \sum_{m<l} f(d_{lm}), \tag{14}$$

where $\{X_l\} = \{X_1, \ldots, X_L\}$ is a set of L symbols, and d_{lm} is the Euclidean distance between symbols $X_l = \{x_{l1}, \ldots, x_{lN}\}$ and $X_m = \{x_{m1}, \ldots, x_{mN}\}$

$$d_{lm} = \left[\sum_{j=1}^{N} (x_{lj} - x_{mj})^2 \right]^{\frac{1}{2}}, \tag{15}$$

where it is assumed that $\|X_l\| = 1$, $\forall l$ $(l = 1, \ldots, L)$. Function f is an arbitrary monotonically decreasing convex function with continuos first and second derivatives over the interval $(0, d_{lm\ max})$, where $d_{lm\ max}$ is the maximum Euclidean distance between symbols belonging to $\{X_l\}$ [11]. For $f(d_{lm}) = d_{lm}^{-a}$, $a > 0$, the iterative method, slightly modified in order to encompass the constraint (13), can be restated as

$$X_l^{(k+1)} = X_l^{(k)} + \alpha \sum_{m \neq l} \frac{X_m - X_l}{d_{lm}^{\nu}}, \tag{16}$$

$$X_{lj}^{(k)} = \frac{X_{lj}}{|X_{lj}|}\frac{1}{\sqrt{n}} \qquad l = 1, 2, \dots, M; \quad j = 0, \dots, n-1, \tag{17}$$

where $\nu = a + 2$, and $X_{lj} = [x_{l3j+1}\ x_{l3j+2}\ x_{l3j+3}]$.

Minimum Euclidean distances for the optimized 3–D, 6–D, 9–D, and 12–D signal point constellations, for $k = 1$ and $k = 2$, are given in Table 1.

Table 1. Minimum euclidean distance d_{min} in the optimized $3n$–dimensional constellations with L signal points

The number of dimensions D	$k=1$		$k=2$	
	L	d_{min}	L	d_{min}
3	2	2	4	1.633
6	4	1.633	16	1.271
9	8	1.512	64	1.140
12	16	1.414	256	1.039

Decoding of $3n$–dimensional POLSK signals could be simplified in the case of regular placement of signal points. Lattice codes have the symmetry that allows construction of certain decoding rules, which yield lower complexity decoders.

For obtaining regular signal point constellations, we used the lattice packing E_6 with the generator matrix given in [6].

A software routine was devised which, at a given squared distance m from the origin, extracts all lattice points satisfying the condition (13). All possible permutations of the generator matrix columns are included. 6–D signal points obtained in this way have perfect symmetry.

As an example, a signal point constellation obtained from E_6 with $m = 8$ is shown in Fig. 4. Signal points are composed of different combinations of 3–D points lying on the first and the second sphere. Each 3–D point represents a polarization state. This 6–D constellation has 360 signal points. A code can be constructed by extracting the appropriate subset consisting of the desired number of signal points. The best subset of sixteen 6–D signal points extracted from the constellation shown in Fig. 4. has the minimum Euclidean distance $d_{min} = 1.225$, while for the best possible arrangement, $d_{min} = 1.271$.

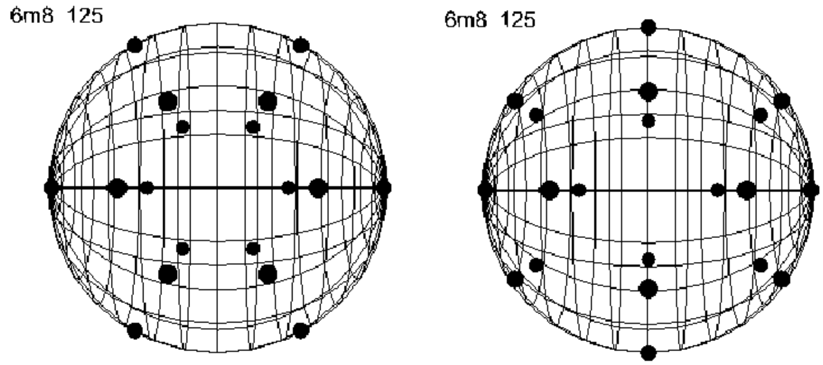

Figure 4. 6–D constellation of 360 signal points obtained from the E_6 lattice packing at the squared distance $m = 8$ from the origin. A signal point is represented as a combination of the two 3–D points.

5. Simulation model

In [12] we have proposed a simulation method for POLSK systems based on the vector model of the optical channel. Here we extend the same method to $3n$ dymensional space. Coherent detection (CD) of POLSK signals is assumed. Obtained results are also applicable to direct detection systems, if the amplified spontaneous emission noise (ASE) is the prevailing noise. The latter is always true in long haul optically amplified direct detection systems.

The electric field vector of the eliptically polarized lightwave can be presented as

$$E = A(\cos \alpha i_x + e^{-j\delta} \sin \alpha i_y). \tag{18}$$

According to (2) we obtain the Stokes parameters in the following form

$$s_0 = A^2, \tag{19a}$$

$$s_1 = A^2 \cos 2\alpha, \tag{19b}$$

$$s_2 = A^2 \sin 2\alpha \cos 2\delta, \tag{19c}$$

$$s_3 = A^2 \sin 2\alpha \sin 2\delta. \tag{19d}$$

From (19a) i (19b) it follows that

$$\alpha = \frac{1}{2} \arccos \frac{s_1}{s_0}. \tag{20}$$

According to (19c) i (19d), and limiting the value of atan function to the interval $[-\pi/2\ \pi/2]$, we obtain

$$\delta = \begin{cases} \arctan \dfrac{s_3}{s_2} + \pi, & s_2 < 0; \\ -\dfrac{\pi}{2}, & s_2 = 0, s_3 < 0; \\ \dfrac{\pi}{2}, & s_2 = 0, s_3 > 0; \\ \arctan \dfrac{s_3}{s_2}, & s_2 > 0. \end{cases} \tag{21}$$

In the case $s_2 = s_3 = 0$, the value of δ is not important. For every input SOP vector (s1, s2, s3), using (20) and (21) we calculate the electric field components as

$$\begin{aligned} E_x &= A \cos \alpha, \\ E_y &= A e^{-j\delta} \sin \alpha. \end{aligned} \tag{22}$$

Signals in two orthogonal channels of the POLSK receiver are

$$\begin{aligned} v_x &= E_x + n_1 + jn_2, \\ v_y &= E_y + n_3 + jn_4, \end{aligned} \tag{23}$$

where n_1, n_2, n_3 and n_4 are independent Gaussian noise processes, which originate from the local oscillator shot noise after IF filtering in the coherent receiver. In the case of direct detection these noise processes represent the filtered ASE noise. The influence of the laser phase noise is not included, as it can be successively canceled out with wide enough filtering followed by a postdetection filter [5]. An eficient simulation method that accounts for the laser phase noise is presented in [8]. The estimates of the Stokes parameters are found using

$$\begin{aligned} \tilde{s}_1 &= |\nu_x|^2 - |\nu_y|^2, \\ \tilde{s}_2 &= \nu_x \nu_y^* + \nu_x^* \nu_y, \\ \tilde{s}_3 &= j(-\nu_x \nu_y^* + \nu_x^* \nu_y). \end{aligned} \tag{24}$$

To decide which symbol was transmitted we apply scalar product of the estimated $3n$ dimensional vector with all the possible symbols. The decision is made according to the maximum dot product.

In simulations we used the importance sampling technique [13]. This technique makes the occurence of the rare error events more frequent and thus saves computational time. When the signal–to–noise ratio is high, instead of the real probability density function (pdf) f with variance σ^2, we use a modified pdf f^* with variance σ^{*2}. The correction factor while counting the number of error events, for $3n$ dymensional symbols, is

$$\omega = \prod_{j=1}^{n} \frac{f(n_{1j})f(n_{2j})f(n_{3j})f(n_{4j})}{f^*(n_{1j})f^*(n_{2j})f^*(n_{3j})f^*(n_{4j})} \tag{25}$$

If we take into account that f and f^* in (25) are normal pdf's with variances σ^2 and σ^{*2} respectively, we obtain

$$\omega_k = \left(\frac{\sigma^*}{\sigma}\right)^{4n} e^{-\left(\frac{1}{2\sigma^2}-\frac{1}{2\sigma^{*2}}\right)\sum_{j=1}^{n}(n_{1j,k}^2+n_{2j,k}^2+n_{3j,k}^2+n_{4j,k}^2)} \tag{26}$$

where ω_k is the correction factor for the k–th error event, and $n_{ij,k}$ represents the realization of the process $n_{ij,}$, which contributed to the k–th error event.

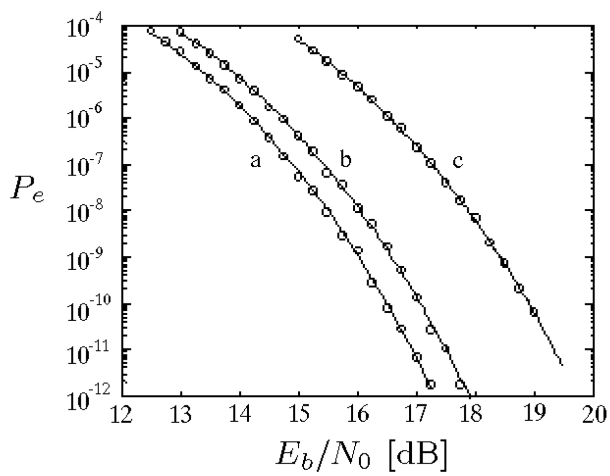

Figure 5. The error probability versus signal to noise ratio per transmitted bit. Solid lines – analytical results, circles – simulation results. a) binary POLSK, b) 4–POLSK tetrahedron, c) 8–POLSK cube.

In Fig. 5. we compare simulation results for regular 3–dymensional constellations, with the analytical ones, obtained by applying Eqs. (8)-(11).

6. Simulation results

Simulation results for transmission of $k = 1$ bit per signaling period, with optimum $3n$–D signal point constellations are shown in Fig 6. Similar results, shown in Fig. 7. correspond to $k = 2$. The error probability P_e is plotted against the signal to noise ratio per transmitted bit

$$\frac{E_b}{N_0} = \frac{\frac{E}{N_0}}{\log_2 M} = \frac{1}{\log_2 M}\frac{s_0}{2\sigma^2}, \tag{27}$$

where $M = 2^k$ and s_0 is the fourth Stokes parameter, equal to the optical signal power in the case of a fully polarized lightwave. σ^2 is the variance of additive Gausian noise, appearing in each of the two orthogonal components of the received signal. In this way, different $3n$–dimensional signal point constellations can be compared, while the bit rate and the bandwidth occupation are fixed.

For $k = 1$, the optimised 6–D signal point constellation offers no significant gain with respect to antipodal 3–D case. However, with 9–D and 12–D constellations the potential gain with respect to the 3–D case, at $P_e = 10^{-9}$ is around 0.3dB and 0.9dB, respectively.

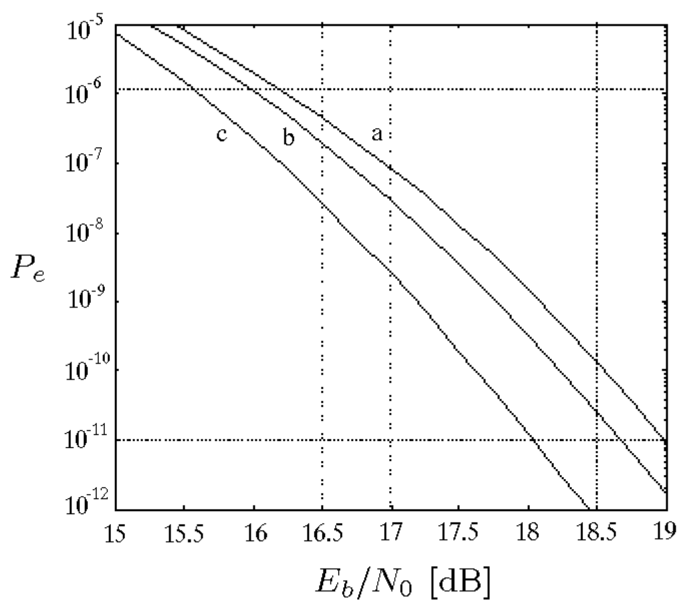

Figure 6. Simulation results for the error probability vs. signal–to–noise ratio per transmitted bit. The transmission of $k = 1$ bits per signaling period, with optimum 3n-D signal point constellations a) 3–D (antipodal), b) 9–D, and c) 12–D.

For $k = 2$, higher gain is achieved by increasing signal space dimensionality. 6–D optimized constellation with 16 signal points is better than 3–D tetrahedron for about 0.4 dB, at $P_e = 10^{-9}$. With 9–D optimized constellation a gain of 0.9 dB is achieved, while 12–D constellation offers a gain of around 1.3 dB with respect to 3–D tetrahedron.

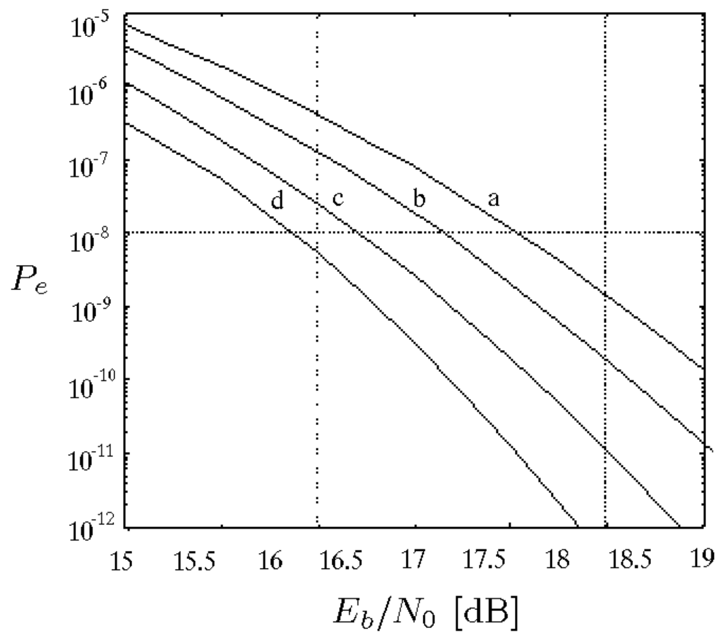

Figure 7. The same as Fig. 6. but for $k = 2$ bits per signaling period. a) 3–D (tetrahedron), b) 6–D, c) 9–D, and d) 12–D.

Simulation results for error probability, corresponding to transmission of $k = 3$ bits per signaling period are shown in Fig. 8. The optimum 3–D and 6–D signal point constellations are considered. For 3–D optimum arrangement of 8 points, $d_{min} = 1.216$, while for the optimized 6–D arrangement of 64 points, $d_{min} = 0.946$. The error probability for 3–D cube is also shown for comparison. For $k = 3$, 6–D constellation offers a gain of about 0.7 dB with respect to the optimum 3–D constellation and about 1.25 dB with respect to 3–D cube. Comparing the results on Figs. 6, 7 and 8, it can be seen that for a grater number of bits per signaling period, the increase in the signal space dimensionality results in a higher gain.

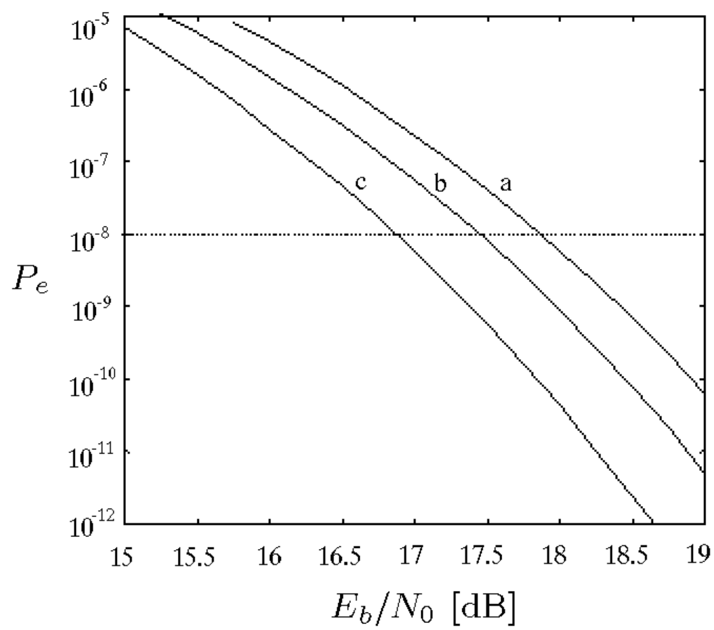

Figure 8. The same as Fig. 6. but for $k = 2$ bits per signaling period. a) 3–D cube, b) 3–D optimum constellation with 8 signal points, and c) 6–D optimized constellation with 64 signal points.

7. Conclusion

A potential improvement in POLSK systems performance, resulting from increased dimensionality of signal space, is investigated through simulation. Signal point constellations were optimized in a way that maximizes the minimum squared Euclidean distance, while preserving the constant power signaling. The gain in system performance is achieved at the expense of an increased complexity at the receiver. In order to lower the decoder complexity, signal point constellations with perfect symmetry could be extracted from an appropriate lattice.

REFERENCES

1. S. Benedetto, P. Poggiolini: *Theory of Polarization Shift Keying Modulation.* IEEE Trans. Commun., vol. 40, no. 4, pp. 708–721, Apr. 1992.
2. S. Benedetto, P. Poggiolini: *Multilevel Polarization Shift Keying: Optimum Receiver Structure and Performance Evaluation.* IEEE Trans. Commun., vol. 42, no. 2/3/4, pp. 1174–1186, Feb./Mar./Apr. 1994.

3. S. Betti, G. De Marchis, E. Iannone: *Polarization Modulated Direct Detection Optical Transmission Systems.* J. Light. Technol., vol. 10, no. 12, pp. 1985–1997, Dec. 1992.
4. R. Blaikie, D.P. Taylor, P.T. Gough: *Multilevel Differential Polarization Shift Keying.* IEEE, Trans. Commun., vol. 45, no. 1, pp. 95–102, Jan 1997.
5. S. Benedetto, R. Gaudino, P. Poggiolini: *Performance of Coherent Optical Polarization Shift Keying Modulation in the Presence of Phase Noise.* IEEE Trans. Commun, vol. 43, no. 2/3/4, pp. 1603–1612, Feb./Mar./Apr. 1995.
6. N.J.A. Sloane: *Tables of Sphere Packings and Spherical Codes.* IEEE, Trans. on Inform. Theory, vol. IT–27, no. 3, pp. 327–338, May 1981.
7. M. Born, E. Wolf: *Principles of Optics.* Pergamon Press, 1964.
8. A. Pižurica: *Signal Transmission in Optical Systems with Polarization Shift Keying Modulation.* Master Thesis, Belgrade, 1997.
9. E. Iannone, F. Matera, A. Mecozzi, M. Settembre: *Performance Evaluation of Very Long Span Direct Detection Intensity and Polarization Modulated Systems.* IEEE, J. Lightwave Technol., vol. 14, no. 3, pp. 261–272, March 1996.
10. I.P. Kaminow: *Polarization in Optical Fibers.* IEEE, J. Quantum Electron., vol. QE–17, no. 1, pp. 15–22, Jan. 1981.
11. D.E. Lazić, V. Š enk, I.P. Š eš kar: *Arrangements of Points on a Sphere which Maximize the Least Distance.* Bulletins for Applied Mathematics, Vol. XLVII, No. 479/87, pp. 7–21, Technical University Budapest, August 1987.
12. A. Pižurica, V. Šenk, M. Despotović, A. Marinčić: *Simulacioni model optičkog sistema sa polarizacionom modulacijom.*, ETRAN'97.
13. M. Jeruchim: *Techniques for Estimating the Bit Error Rate in the Simulation of Digital Communication Systems.* IEEE, JSAC, vol. SAC 2, no. 1, pp. 158–170, Jan. 1984.